Author/s:
Javadi, M;Gu, Q;Naficy, S;Farajikhah, S;Crook, JM;Wallace, GG;Beirne, S;Moulton, SE

Title:
Conductive Tough Hydrogel for Bioapplications

Date:
2018-02-01

Citation:
Javadi, M., Gu, Q., Naficy, S., Farajikhah, S., Crook, J. M., Wallace, G. G., Beirne, S. & Moulton, S. E. (2018). Conductive Tough Hydrogel for Bioapplications. Macromolecular Bioscience, 18 (2), https://doi.org/10.1002/mabi.201700270.

DOI: 10.1002/marc.((insert number)) ((or ppap., mabi., macp., mame., mren., mats.))

Article Type ((Full Paper))

Conductive Tough Hydrogel for Bio-applications

*Mohammad Javadi, Qi Gu, Sina Naficy, Syamak Farajikhah, Jeremy M. Crook, Gordon G. Wallace, Stephen Beirne and Simon E. Moulton**

Mohammad Javadi, Qi Gu, Syamak Farajikhah, Associate Prof. Jeremy M. Crook, Prof. Gordon Wallace, Dr. Stephen Beirne
ARC Centre of Excellence for Electromaterials Science, Intelligent Polymer Research Institute, University of Wollongong, Wollongong, NSW 2522, Australia
Dr. Sina Naficy
School of Chemical and Biomolecular Engineering, The University of Sydney, Sydney, New South Wales 2006, Australia
Qi Gu
State Key Laboratory of Stem Cell and Reproductive Biology, Institute of Zoology, Chinese Academy of Sciences, Beijing, 100101, P.R. China
Assoc. Prof. J. M. Crook
Illawarra Health and Medical Research Institute, University of Wollongong, Wollongong, New South Wales 2522, Australia
Assoc. Prof. J. M. Crook
Department of Surgery, St Vincent's Hospital, The University of Melbourne, Fitzroy, Victoria 3065, Australia
Prof. Simon E. Moulton
ARC Centre of Excellence for Electromaterials Science, Faculty of Science, Engineering and Technology, Swinburne University of Technology, Hawthorn, Victoria 3122, Australia

Abstract

Biocompatible conductive tough hydrogels represent a new class of advanced materials combining the properties of tough hydrogels and biocompatible conductors. Here we report a simple method, to achieve a self-assembled tough elastomeric composite structure that is biocompatible, conductive, and with high flexibility. The hydrogel comprises polyether-based liner polyurethane (PU), poly (3,4-ethylenedioxythiophene) (PEDOT) doped with poly(4-styrenesulfonate) (PSS) and liquid crystal graphene oxide (LCGO). The polyurethane hybrid

composite (PUHC) containing the PEDOT:PSS, LCGO, and PU has a higher electrical conductivity (10×), tensile modulus (>1.6×) and yield strength (>1.56×) compared to respective control samples. Furthermore, the PUHC is biocompatible and can support human neural stem cell (NSC) growth and differentiation to neurons and supporting neuroglia. Moreover, the stimulation of PUHC enhances NSC differentiation with enhanced neuritogenesis compared to unstimulated cultures. A model describing the synergistic effects of the PUHC components and their influence on the uniformity, biocompatibility and electromechanical properties of the hydrogel is presented.

Keywords

conductive hydrogel, neural stem cells, graphene, PEDOT:PSS, polyurethane

1. Introduction

Over the last two decades, conductive hydrogels have attracted much interest for both academic research and commercial application. Hydrogels are polymeric materials, with a hydrophilic structure that renders them capable of holding large amounts of water or other polar solvents in their 3D networks.[1] Conductive hydrogels incorporate an additional functionality by enabling the conduction of electricity. Such materials have great potential for use in wearable and implantable sensors for healthcare, mimicry of neural networks, soft robotics, and electro-stimulated drug release.[2-5]

Electrically conductive hydrogels have previously been produced by combining a hydrophilic matrix with conductive fillers[6] such as metallic particles, conductive polymers (CP), or carbon-based fillers.[7-9] Composite materials of a polymeric matrix and randomly dispersed metal particles are considered as heterogeneous disordered systems and have low durability.[9] Among all CPs, potentially PEDOT:PSS is the most promising because of its

dispersibility (high stability in its p-doped form) in polar solvents and hence excellent processability, and the high conductivity, attainable. Therefore, PEDOT: PSS has been widely used as a conductive component in many hybrid systems to enhance electrical conductivity.[10-11] In this regard, the discovery of graphene and its derivatives has opened new pathways for developing conductive composites. Graphene-based fillers have a high surface area, large aspect ratio, and both excellent thermal and electrical conducting properties that can be imported to composites containing them.[12] The antibacterial activity of graphene and its derivatives make it appealing for biomedical application.[13-14] Notwithstanding, it is technically impractical to produce scaffolds solely from graphene[15], and so graphene-based fillers are typically dispersed in processable polymers.[16]

Although graphene sheets exhibit high in-planar (intra-sheet) electrical conductivity, their trans-planar (inter-sheet) conductivity greatly diminishes for low loading of graphene in an insulating matrix. The efficiency of charge transfer between adjacent sheets is normally limited by the insulating coating of the graphene sheets by the matrix material. While the problem can be addressed by increasing the ratio of fillers to the matrix, this in turn negatively impacts on the matrix flexibility and stretchability whereby the hydrogel composites are brittle, possess relatively low flexibility and are unable to undergo elongational deformations.[17]

In the human body, endogenous electric fields generated from the membranes of cells serve as important cues to direct cell migration during embryonic development and wound healing.[18] Accordingly, it has been well documented that externally applied electric fields during cell culture can improve the growth of electro-responsive cells such as nerve and muscle cells.[19] Electrically stimulated tissue engineering is dependent on the identification and development of novel electrode materials that are processable, electrochemically stable,

soft, and biocompatible.[20-22] Studies have shown that hybrid hydrogels encapsulating electrospun fibres coated with conducting polymer demonstrated improved mechanical and conductive properties and that these materials are suitable for axonal growth and neural tissue engineering.[23-24] However, the development of an easy to produce conductive and biocompatible hydrogel with the ability to sustain large dimensional deformations without any mechanical failure, while remaining stable in aqueous and dry ambient conditions has proved challenging. Consequently, progress in the field has been slow with the limited development of conductive hydrogel formulations that contain well-dispersed conducting fillers.

Here we report the production of an electrical conducting tough polyurethane hybrid composite (PUHC) hydrogel by a simple method that possesses excellent mechanical performance and biocompatibility. The PUHC is made from well-dispersed PEDOT:PSS, liquid crystalline graphene oxide (LCGO) and a hydrophilic polyurethane matrix (PU). The optimized formulations used to prepare the PUHC are easy to process via solution casting to produce films with high conductivity and stretchability. Biocompatibility is demonstrated through culture and differentiation of clinically-relevant human neural stem cells (hNSCs) to neurons and supporting neuroglia on the films, with electrical stimulation enhancing neuritogenesis.

2.Experimental

2.1 Materials

Expandable graphite used as the precursor for synthesizing ultra-large GO sheets was obtained from Asbury Carbon (3772). LCGO dispersions were prepared following the process outlined previously.[25] Orgacon™ DRY re-dispersible PEDOT: PSS pellets were

from Agfa. Ethanol and DMF were purchased from Sigma-Aldrich and used as supplied. HydroMed D3 (AdvanSource, USA; referred to as PU-D3 hereafter) was used as the base polyurethane material (PU-D3). Hypophosphorous acid (H_3PO_2) that was used as a reduction agent was obtained from Sigma-Aldrich as a 50 wt. % solution in water and used as received. All chemicals were analytical grades, and their solutions were prepared using Milli-Q water (18.2 MΩ) (Nanopure water, Barnstead).

2.2 Composite solution preparation and film casting

For making LCGO dispersions in ethanol (EtOH), 10 ml of the stock aqueous LCGO was poured into a 50 ml centrifuge tube (Nalgene, Thermofisher, USA) to which 20 ml of the EtOH was added and then mixed vigorously by vortex shaking. After centrifugation, 30 ml of the supernatant was extracted, replaced with 30 ml of the EtOH and then mixed vigorously by vortex shaking. This process was repeated 10 times to replace the water with the EtOH. PU/LCGO/PEDOT: PSS composite (PUHC) formulations were prepared as follows: various amount of LCGO dispersion in EtOH were added to a 1:1 mixture of DMF and water. PEDOT:PSS (10 mg ml^{-1}) was then added to this mixture. Separately, PU-D3 solution (5 % w/w) was achieved by dissolving PU in a 95:5 mixture of EtOH: water. This PU-D3 solution was added to the LCGO/PEDOT:PSS dispersion in DMF:water. With the final concentration of PU in this mixture was 92 % w/w. Subsequently, the mixtures were stirred by a vortex mixer (45 °C for 24 h) in a round-bottom flask. Hydrogel films were prepared via solution casting of these formulations in glass Petri dishes. Solvents were removed using a vacuum oven (70 °C, -80 Kpa, 12 h) to obtain uniform films. After evaporation of solvent mixture, films were rehydrated by adding water on top of the films, allowing them to fully swell and release from the Petri dish.

The reduction of the PUHC films was carried out by immersing the hydrogel films into a 5% aqueous solution of H_3PO_2 acid (50 °C for 12 h) in a round-bottom flask. Afterward, samples were then thoroughly rinsed with Milli-Q water to remove the remaining acid (wash cycle was 10 times 30 min each cycle).

2.3 Characterization

Raman spectroscopy was carried out on composite films using a Jobin Yvon Horiba HR800 Raman microscope, utilizing a 632 nm laser line and a 300-line grating. X-ray diffraction (XRD) analysis of the composite films was conducted using GBC MMA diffraction instrument (GBC Scientific Equipment Pty Ltd, Australia) equipped with Cu-Kα radiation. The mechanical properties of dry composite films and wet composite films were tested using a Shimadzu mechanical tester (EZ-L). Samples for mechanical testing were prepared by laser cutting the films (Versa Laser VLS4.60) into strips of 5 mm wide and 15 mm long. The tensile properties of sample strips were measured at a constant strain rate of 0.01 mm min^{-1}, and tests were performed on at least 6 samples cut from each cast film. The tensile strength, elongation at break and Young's modulus were reported as the average of all measurements. Scanning electron microscopy (SEM) images were taken with a field-emission SEM instrument (JEOL JSM-7500FA). Samples were frozen in liquid nitrogen, fractured and sputter-coated (EDWARDS Auto 306) with a thin layer of gold (12 nm thickness). LCGO samples for measuring average sheets size via SEM image were prepared by depositing LCGO sheets on a silanized silicon wafer (300 rims SiO2 layer) to ensure good adhesion. Silane solution was prepared by mixing (3-aminopropyl) trimethoxysilane (Sigma-Aldrich) with Milli-Q water (1:9 v/v) followed by addition of 30 µl hydrochloric acid (32%, Sigma-Aldrich). After washing with water and EtOH and drying at room temperature, the silicon wafer was silanized by immersing it in the silane solution for 30 min followed by washing

with Milli-Q water and drying at room temperature. The wafer was dried at laboratory temperature before SEM analysis. The bulk conductivity of the samples was measured by a two-point probe method using a multimeter (Fluke 287 True-RMS). The conductivity was then calculated using the following equation:

$$\rho = R\frac{A}{l} \quad (1)$$

$$\sigma = \frac{l}{\rho} \quad (2)$$

Where ρ is the resistivity (Ω/□), R is the resistance (Ω), A is the cross-sectional area of the specimen (cm), l is the length of the specimen (cm), and σ is the conductivity (S cm^{-1}).

The water content was calculated as follows:

$$\text{water content (\%)} = \frac{(Wo-W)}{Wo}\ x\ 100\% \quad (3)$$

Where *Wo* and *W* are the weight of the films before and after drying respectively.

2.4 Cell culture and differentiation

Working stocks of human neural stem cells (hNSCs, ReNcell CX, SCC007, Millipore) were maintained under 5% CO2, seeding at a density of 2 – 3 x 10^6 cells in self-renewal medium consisting of NeuroCult NS-A (#5751, Stem Cell Technologies) with 2µg/ml Heparin (Sigma), basic fibroblast growth factor (FGF2, 20ng/ml; Peprotech) and epidermal growth factor (EGF, 20ng/ml; Peprotech) on laminin (Life Technologies) coated 6-well plates (Greiner Bio-One). Cells were passaged every 5-7 days by digesting in Triple (Life Technologies) for 3 min at 37°C. hNSCs were similarly cultured on G-film that was fixed to the bottom of culture plate wells. Differentiation of hNSCs was performed in a differentiated neural medium comprising 2 parts DMEM F-12: 1 part Neurobasal supplemented with 0.5%

N2 (Gibco), 2% StemPro (Life Technologies) and 50 ng/mL brain-derived neurotrophic factor (BDNF; Peprotech) for 7 days.

2.5 Electrical stimulation

hNSCs were seeded on PUHC within a 4-well culture chamber customized for concomitant electrical stimulation (Supplemental Figure 1). Cells were seeded at a density of $5x10^4$ cells/cm^2 in self-renewal medium, allowed to adhere for 24 h, and subsequently stimulated for 8 h per 24 h at 37°C under CO_2 for 3 days. The stimulation paradigm was ±0.25 mA/cm^2 using a biphasic waveform of 100 μs pulses with 20 μs interphase at 250Hz on a Digital Stimulator DS8000 and A365 Isolator units (World Precision Instruments) interfaced with an e-corder system (eDAQ)[12]. Stimulation was performed in self-renewal medium to determine an effect independent of standard medium-directed differentiation on hNSC-neuritogenesis.

2.6 Immunocytochemistry and analysis

Cell samples were fixed with 3.7% paraformaldehyde solution in PBS for 10 min and then blocked and permeabilized in 0.3% Triton X-100 containing 10% donkey serum for 1h at 37℃. The cells were incubated with primary antibodies against SOX2 (1:500, rabbit; Millipore), Vimentin (1:1000, chicken; Millipore), TUJ1 (1:1000, chicken; Millipore) or glial fibrillary acidic protein (GFAP, 1:1000, rabbit; Millipore) overnight at 4℃. After rinsing with PBS containing 0.1% Triton X-100, the samples were incubated with Alexa 647, 594 or 488 (1:1000; Invitrogen) secondary antibody for 1h at room temperature (RT). A further wash was undertaken followed by 5 min incubation at RT with 1 mg/mL DAPI in PBS. Imaging was performed using a Leica confocal microscope (Leica TSC SP5 II), and neurite studies were completed using MetaMorph software V 7.8 with the neurite analysis plugin. Vimentin labeling was employed for neurite studies representative of early-stage neuritogenesis.

3. Results and Discussion

Stable dispersions of PEDOT: PSS, LCGO, and PU were prepared by dissolving PEDOT:PSS in water and DMF (50:50), followed by addition of LCGO dispersion in ethanol (EtOH) and PU (for more details see Experimental section). The difference in dispersibility of PU, LCGO, and PEDOT: PSS in various organic solvents is expected to influence the ability to prepare homogeneous PUHC formulations for composite film formation purposes. DMF and EtOH solvents provided the best dispersibility for both PU and PEDOT:PSS and were therefore used to compare the processability of the composite formulations. The use of DMF and water in making PEDOT:PSS formulations resulted in dispersions that are stable for one month and displayed a higher electrical conductivity than that of the equivalent dispersion prepared in water. The addition of PEDOT:PSS and LCGO to PU dispersions resulted in homogeneous PUHC formulations that were stable for at least six months after preparation (Figure 1a). The x-ray diffraction (XRD) results in **Error! Reference source not found.** reveal that XRD patterns of PUHC do not show any characteristic signals for LCGO. This lack of XRD signal may be due to the high dispersion of graphene sheets within PU matrix.

Free standing reduced PUHC films were prepared by incorporating a range of filler (PEDOT: PSS/LGOC at 1:1 ratio) % w/w into the PU (in a solvent mixture of ethanol, water, and DMF) followed by casting the reduction as described in the experimental section. The electrical and mechanical properties of these films are presented in

Figure **2** and show that the electrical conductivity of the PUHC increases with increasing filler ratio, indicating enhanced electrical conductivity of PUs. It can also be seen that the

toughness of the PU is increased and reaches a maximum at an incorporation of 8 % w/w of filler. Therefore 8 % w/w ratio of filler was chosen as optimal weight percent for further PUHC formulation evaluation. These PUHC films displayed flexibility and were stretchable after solvent removal as is evident from the digital photographs and movies supplied as supporting information (**Error! Reference source not found.**).

3.1 Mechanical Characterisation

Typical stress-strain curves of the PUHC and control samples are presented in Figure 3a and shows the improvement in the tensile modulus, and yield strength but a decrease in elongation at break compared to the PU, PU-LCGO, and PU-PEDOT:PSS film. The data in Table 1 summarizes that the average tensile modulus and yield strength rather than control samples (with the same ratio of fillers) are greater than the control samples by a factor of approximately 1.6 times.

The elastomeric properties of PU and its composites are derived from the presence of the hard and soft copolymer segments of the polymer chains (Figure 3b). The soft segments, which are normally linear chains in their rubbery state (glass transition temperature (T_g) lower than room temperature), are flexible and mobile. These flexible segments are covalently coupled to the hard segments (T_g above room temperature) via urethane linkages (R-NH-CO-O-). When stress is applied to the PU composites, a portion of the soft segments is stressed by uncoiling, and the hard segments become aligned in the stress direction. Therefore, the soft segments provide high elongation while hard segments provide stiffness in PUHC. Previous work has shown that growth in hard segment content gives rise to an increase in tensile modulus, ultimate strength and yield strength, and a decrease in elongation

at break.[25, 26] After adding each of the components to the PU, an increase in tensile strength was observed (**Table 1**) that agrees with other published results.[26-28]

3.2 Electrical conductivity

The electrical conductivity of PUHC films was investigated (Figure 4). The onset of conductivity occurred at ~ 3.8, 2.2 and 1.7 % w/w loadings of PEDOT:PSS, LCGO, and PEDOT:PSS/LCGO (1:1) respectively, above these loadings the composite conductivity increased almost monotonically with filler loading. PUHC (Figure 4c) showed an increase in conductivity after addition of 1.7 % w/w of a 1:1 blend of PEDOT:PSS and LCGO. This correlates to an individual filler content of 0.85 % w/w PEDOT:PSS and 0.85 % w/w LCGO. These values are lower than the individual amounts of 3.8 % w/w and 2.2 % w/w indicated above for PEDOT:PSS and LCGO respectively and indicates a synergistic effect when these two fillers are combined that facilitates an increase in composite conductivity. The conductivity of our optimal PUHC composite is compared to previous reports of conducting PU composites in Table 2. The increase in conductivity may be due to the establishment of LC structure in PUHC (transfer isotropic to nematic structure).[29] Percolation threshold results comparing the electrical behavior of LCGO and PEDOT:PSS/LCGO composites suggested that lower amounts of filler are needed to create conducting paths in an isolating matrix of PU. At ratios below the percolation threshold, the composite conductivity is almost the same as the polymer matrix, and therefore charge carrier transport cannot occur. By increasing the filler loading, the average distance between conducting filler particles decreases and below a certain threshold, charge carrier transport can occur via electrical field assisted tunneling or hopping between neighboring fillers.[30] At the percolation threshold, the amount of filler is enough to begin the formation of a continuous conductive network

throughout the polymer matrix. Furthermore, the combination of PEDOT:PSS and LCGO as conductive fillers offers an attractive route to enhancing electrochemical performance based on morphological modification or electronic interaction between PEDOT:PSS and LCGO. It has been shown (Figure 4a and 4b) that composites based on PEDOT:PSS and LCGO exhibit electrical properties of each of the individual components with the conductivity of PEDOT:PSS much greater than LCGO. It follows that composite production using PEDOT:PSS and LCGO (Figure 4c) reduces the resistive barrier between the conducting fillers and the PU and maximizes the electron transport to improve the conductivity performance.

As indicated above PU polymer chains have hard and soft segments. (Figure 1b) The urethane hard segment domains are physically cross-linked via hydrogen bonding between the amorphous polyether soft segment domains. The mechanism for PU hydrogel cross-linking has been proposed previously in the literature.[31] The latter polyether segments define the amount of water that the PU can hold since they are hydrophilic and therefore able to retain water. While the water content of pure PU is close to 60%, this gradually decreases by the addition of other less hydrophilic components (Figure 5a). It is well documented that the water content has a positive effect on elongation at break and negative effects on tensile modulus, ultimate strength, and yield strength.[41] The data presented in Table 1 is in agreement (within the error range) of this phenomenon. Interactions between the filler and PU were investigated by forming free-standing films and observing their behavior in an EtOH:water (95:5%) solvent. It was found that neither PU/LCGO or PUHC were soluble in the solvent, while both pure PU and its composite with PEDOT:PSS were readily soluble (Figure 5b). This observation indicates that the addition of LCGO prevents the PU chains

from dissolving in its solvent. This effect is most likely due to the documented interaction between LCGO and the hard segment of PU.[26]

The liquid crystal (LC) nature of our materials (Figure 6) provides the ability to have the fillers aligned and maintain an alignment between LCGO nanosheets within the composite that has been shown to result in increased mechanical [26] and electrical [12] properties. The LC phases may offer a dynamic anisotropicity at molecular scale [42] as it is pivotal to control the orientation and spatial ordering of graphene sheets in a precise manner [29] in order to translate individual graphene sheet into high-performance macroscopic materials. The LCGO dispersions in ethanol exhibited a nematic liquid crystalline phase at concentrations above 1.5 % w/w. We found the minimum concentration of LCGO that is required to obtain LC structure in PUHC solution to be approximately 4% w/w (Figure 6). This increase in LCGO concentration required to invoke LC structure may be due to the forces imposed on the LCGO by the PU that prevents the spontaneous formation of LC domains at lower concentrations. The data in Figure 6 suggests that once a critical concentration of LCGO is incorporated these restrictive forces are overcome.

The SEM image shown in Figure 7a illustrates the uniformity of PUHC surface and layered microstructure of composite across the cross section (Figure 7b). This highlights the aligned structure of LCGO nanosheets within the PUHC. The LC structure of graphene causes the sheets to reassemble forming a sandwich structure in the polymer matrix (Figure 7b). The PEDOT:PSS phase is believed to be dispersed between these parallel nanosheets, which can explain the synergistic effect of LCGO and PEDOT:PSS on conductivity. This ordered structure also helps to explain the higher mechanical properties observed for composites containing LCGO. The nematic orientation of fillers within the PU matrix provides a facile pathway for electrons inside the isolated matrix compared to the isotropic orientation and

explains why PUHC's with self-assembly structure have a lower percolation threshold compared to the control samples (Figure 4).

3.3 Reduction of LCGO

GO can be reduced using a range of techniques, including chemical, thermal and electrochemical means. Some of those techniques can produce highly reduced GO, with high conductivity which is similar to pristine graphene.[43]

Optimization of the conductivity and the mechanical properties of the PUHC was achieved using hypophosphorous acid as the reducing agent (Figure 2).[44] The PUHC became conductive following chemical reduction using 5% v/v hypophosphorous acid at 50°C (Figure S4). From Figure S4 it appears that reduction times greater than 6 h are not necessary as maximum conductivity is reached at this time. It has been reported that the partial removal of PSS, due to the treatment of composite containing PEDOT:PSS with acid, could be considered as another reason for the increase in electrical conductivity of the PUHC.[45]

In the Raman spectra (Figure 8) bands at ~ 1590 cm^{-1} are assigned to the symmetric stretch of C=C. Compared to LCGO, this peak for PUHC is shifted towards a higher frequency from 1588 to 1595 cm^{-1}, suggesting the π-π interaction between LCGO and PEDOT:PSS in PUHC.[46, 47] The ratio of the D band intensity (I_D) to the G-band intensity (I_G) which is called the R values (I_D/I_G), indicates the amount of structural order in graphene oxide. From Figure 8 the R-value of LCGO (1.47) is reduced compared to that of PUHC (1.36) and indicates that graphene sheets within the LCGO are more ordered and some of the sp^2 bonds have been restored.[48]

3.4 hNSCs can be cultured and differentiated on PUHC

The biocompatibility of PUHC with hNSCs was initially tested by evaluating cell viability following 24 h culture (**Figure** 9a, b). Live/dead cell analysis indicated robust cell survival (>80%) similar to standard plate-based controls (**Figure** 9b). Importantly, hNSCs expressed neural stem/progenitor cell markers SOX2 and Vimentin and exhibited small immature and sparsely arranged neurites, typical of hNSC culture (Figure 9c). After two weeks culture under differentiation conditions, cell morphology and immunophenotyping was consistent with advanced neuronal cell induction (**Figure** 9d), with TUJ1 immuno-labelling revealing neurons with extensive networks of neurites, and GFAP labeling indicated supporting neuroglia (**Figure** 9d). These data support PUHC biocompatibility and more specifically hNSC survival, proliferation, and differentiation.

3.5 Electrical stimulation *via* PUHC enhances neuritogenesis of hNSCs

Since electrical signals are implicated in a diversity of biological events, electrically conductive biomaterials are increasingly being used to modulate cell and tissue behavior for research and biomedical applications, including tissue engineering and implantable bio-electrodes.[49] Having initially shown PUHC biocompatibility with hNSCs (**Figure 9**), we next investigated the effect of electrical stimulation *via* the hydrogel on cells. Specifically, consistent with our own previous report of increased hNSC neuritogenesis following electrical stimulation using conductive polymer polypyrrole (PPy)[50], compared to unstimulated controls (**Figure 10a,c**), electrical stimulation of hNSCs *via* PUHC enhanced early neuritogenesis (**Figure 10b,c**), manifest as greater total neurite length, mean neurite length, and maximum neurite length per cell (**Figure 10**c). Data corroborates our initial

PUHC cell-biocompatibility studies, substantiates the use of electroactive-substrates for neural cell support [20, 51], and verifies the application of electroactive-PUHC for tissue engineering where electrical stimulation, mechanical softness and other properties of the biomaterial presently shown are deemed important.

4. Conclusions

As discussed above, our experimental results and theoretical calculations provide evidence for chemical interaction between the fillers (LCGO and PEDOT:PSS) due to the synergistic behaviour in mechanical and electrical properties of PUHC but also shows reasonable response to the cell culture. This phenomenon in PUHC properties can be explained 1) physical influence of the LC structure in the composite solution, 2) chemical interaction between LCGO and PEDOT:PSS and these are as a filler with the PU's hard segment to create a synergic filler impacts on PUHC composite and 3) post-treatment of PUHC by acid agent. This work has demonstrated the production of PUHC with conductivity, stability, and elastomeric and biocompatible features. It could, therefore, be considered for use as an advanced material in wearable bionics and stretchable electronics for mimicry of neural networks, a component of implantable electrochemical biosensors, soft robotics, and electro-stimulated drug release.

Supporting Information

Supporting Information is available from the Wiley Online Library or from the authors.

Acknowledgements

The authors wish to acknowledge funding from the Australian Research Council (ARC) Centre of Excellence Scheme (CE140100012), the use of facilities at the University of

Wollongong Electron Microscopy Centre, and the Australian National Fabrication Facility (ANFF) Materials Node for the provision of materials and processing capabilities. We thank Dr. Patricia Hayes for her assistance with Raman spectroscopy measurements, Mr. Tony Romeo for his invaluable assistance with SEM microscopy. We also thank Dr. Ali Jalili, Dr. Pawel Wagner, Ali Jairani, and Prof. Morteza Aghmesheh for their help and comments towards the manuscript.

[1] E. M. Ahmed, *J. Adv. Res.* **2015**, *6*, 105.
[2] T. Nakamura,T. Yokota,Y. Terakawa,J. Reeder,W. Voit,T. Someya,M. Sekino, IEEE-EMBS **2016,** 485-488
[3] J. Ge, E. Neofytou, T. J. Cahill, R. E. Beygui, R. N. Zare, *ACS Nano* **2012**, *6*, 227.
[4] L. Pan, G. Yu, D. Zhai, H. R. Lee, W. Zhao, N. Liu, H. Wang, B. C.-K. Tee, Y. Shi, Y. Cui, *PNAS* **2012**, *109*, 9287.
[5] Y. Lu, W. He, T. Cao, H. Guo, Y. Zhang, Q. Li, Z. Shao, Y. Cui, X. Zhang, *Sci. Rep.* **2014**, *4*, 5792.
[6] P. Pissis, A. Kyritsis, *Sol. State Ionics* **1997**, *97*, 105.
[7] M. Javadi, S. Naficy, S. Beirne, S. Sayyar, R. Jalili, S. E. Moulton, *Mat. Chem. Phys.* **2017**, *186*, 90.
[8] D. Mawad, A. Lauto, G. G. Wallace, "Conductive polymer hydrogels", in *Polymeric hydrogels as smart biomaterials*, Springer, 2016, p. 19.
[9] G. Psarras, *Composites Part A: applied science and manufacturing* **2006**, *37*, 1545.
[10] D. Yoo, J. Kim, J. H. Kim, *Nano Res.* **2014**, *7*, 717.
[11] R. H. Baughman, A. A. Zakhidov, W. A. De Heer, *Science* **2002**, *297*, 787.
[12] T. Kuilla, S. Bhadra, D. Yao, N. H. Kim, S. Bose, J. H. Lee, *Prog. Poly. Sci.* **2010**, *35*, 1350.
[13] S. Liu, T. H. Zeng, M. Hofmann, E. Burcombe, J. Wei, R. Jiang, J. Kong, Y. Chen, *ACS Nano* **2011**, *5*, 6971.
[14] H. Dong, S. Qi, *Biosurf. Biotrib.* **2015**, *1*, 229.
[15] C. Chung, Y.-K. Kim, D. Shin, S.-R. Ryoo, B. H. Hong, D.-H. Min, *Acc. Chem. Res.* **2013**, *46*, 2211.
[16] Y. Wang, Z. Li, J. Wang, J. Li, Y. Lin, *Trends in Biotech.* **2011**, *29*, 205.
[17] S. Seyedin, J. M. Razal, P. C. Innis, R. Jalili, G. G. Wallace, *Adv. Mater. Interf.* **2016**, n/a.
[18] M. Zhao, *cell & developmental biology*, Elsevier **2009**, p. 20/674.
[19] S. Y. Park, J. Park, S. H. Sim, M. G. Sung, K. S. Kim, B. H. Hong, S. Hong, *Adv. Mater.* **2011**, *23*.
[20] C. E. Schmidt, V. R. Shastri, J. P. Vacanti, R. Langer, *PNAS* **1997**, *94*, 8948.
[21] L. Jin, J. H. Lee, O. S. Jin, Y. C. Shin, M. J. Kim, S. W. Hong, M. H. Lee, J.-C. Park, D.-W. Han, *J. Nanosci. Nanotech.* **2015**, *15*, 7966.
[22] B. Koerbitzer, P. Krauss, C. Nick, S. Yadav, J. J. Schneider, C. Thielemann, *2D Materials* **2016**, *3*, 024004.
[23] M. R. Abidian, D. C. Martin, *Adv. Funct. Mater.* **2009**, *19*, 573.
[24] M. R. Abidian, E. D. Daneshvar, B. M. Egeland, D. R. Kipke, P. S. Cederna, M. G. Urbanchek, *Adv. Health. Mater.* **2012**, *1*, 762.
[25] S. H. Aboutalebi, M. M. Gudarzi, Q. B. Zheng, J.-K. Kim, *Adv. Funct. Mater.* **2011**, *21*, 2978.
[26] D. Cai, J. Jin, K. Yusoh, R. Rafiq, M. Song, *Comp. Sci. Tech.* **2012**, *72*, 702.

[27] H. Saleem, A. Edathil, T. Ncube, J. Pokhrel, S. Khoori, A. Abraham, V. Mittal, *Macromol. Mater. Eng.* **2016**, *301*, 231.
[28] H. Kim, Y. Miura, C. W. Macosko, *Chem. Mater.* **2010**, *22*, 3441.
[29] R. Narayan, J. E. Kim, J. Y. Kim, K. E. Lee, S. O. Kim, *Adv. Mater.* **2016**, *28*, 3045.
[30] N. Hu, Y. Karube, C. Yan, Z. Masuda, H. Fukunaga, *Acta Materialia* **2008**, *56*, 2929.
[31] L. Born, H. Hespe, *Col. Poly. Sci.* **1985**, *263*, 335.
[32] J.-Y. Kwon, E.-Y. Kim, H.-D. Kim, *Macromol. Res.* **2004**, *12*, 303.
[33] Danqing Chen, Guohua Chen, *J. Reinf. Plas. Comp.* **2011**, *30*, 757.
[34] M. Kotal, S. K. Srivastava, B. Paramanik, *J. Phys. Chem C* **2011**, *115*, 1496.
[35] J. W. Cho, J. W. Kim, Y. C. Jung, N. S. Goo, *Macromol. Rapid Comm.* **2005**, *26*, 412.
[36] H.-F. Lee, H. H. Yu, *Soft Mat.* **2011**, *7*, 3801.
[37] G. Carotenuto, V. Romeo, I. Cannavaro, D. Roncato, B. Martorana, M. Gosso, "Graphene-polymer composites", in *IOP Conference Series: Materials Science and Engineering*, IOP Publishing, 2012, p. 40/012018.
[38] S. Shang, W. Zeng, X.-m. Tao, *J. Mat. Chem.* **2011**, *21*, 7274.
[39] P. Puri, R. Mehta, S. Rattan, *J. Electron. Mat.* **2015**, *44*, 4255.
[40] M. Z. Seyedin, J. M. Razal, P. C. Innis, G. G. Wallace, *Adv. Funct. Mater.* **2014**, *24*, 3104.
[41] S. St. Lawrence, J. L. Willett, C. J. Carriere, *Polymer* **2001**, *42*, 5643.
[42] J.-J. Shao, W. Lv, Q.-H. Yang, *Adv. Mater.* **2014**, *26*, 5586.
[43] S. Gambhir, R. Jalili, D. L. Officer, G. G. Wallace, *NPG Asia Mater.* **2015**, *7*, e186.
[44] T. Dutta, R. Sarkar, B. Pakhira, S. Ghosh, R. Sarkar, A. Barui, S. Sarkar, *RSC Adv.* **2015**, *5*, 80192.
[45] S. Khodakarimi, M. Hekhmatshoar, M. Nasiri, M. K. Moghaddam, F. Abbasi, *J. Mater. Sci.: Mater. Elect.* **2016**, *27*, 1278.
[46] Z. Liu, K. Parvez, R. Li, R. Dong, X. Feng, K. Müllen, *Adv. Mater.* **2015**, *27*, 669.
[47] T. Chen, J. Qiu, K. Zhu, J. Li, J. Wang, S. Li, X. Wang, *RSC Adv.* **2014**, *4*, 64061.
[48] D. Yang, A. Velamakanni, G. Bozoklu, S. Park, M. Stoller, R. D. Piner, S. Stankovich, I. Jung, D. A. Field, C. A. Ventrice Jr, R. S. Ruoff, *Carbon* **2009**, *47*, 145.
[49] J. G. Hardy, J. Y. Lee, C. E. Schmidt, *Cur. Op. Biotech.* **2013**, *24*, 847.
[50] C. D. McCaig, A. M. Rajnicek, B. Song, M. Zhao, *Phys. Rev.* **2005**, *85*, 943.
[51] E. Stewart, N. R. Kobayashi, M. J. Higgins, A. F. Quigley, S. Jamali, S. E. Moulton, R. M. Kapsa, G. G. Wallace, J. M. Crook, *Tiss. Eng. C.* **2014**, *21*, 385.

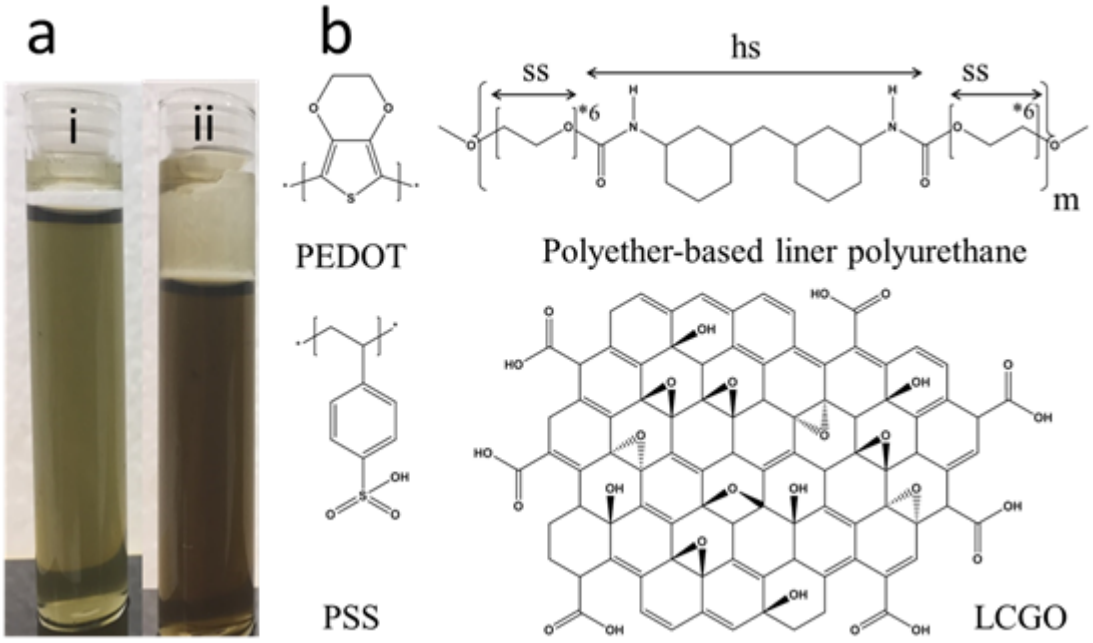

Figure 1 a) Fresh homogeneous PUHC formulations (i) and 6 months after preparation (ii), b) Chemical structure of PEDOT:PSS, LCGO and polyether-based liner polyurethane (abbreviation: ss - soft segment and hs - hard segment).

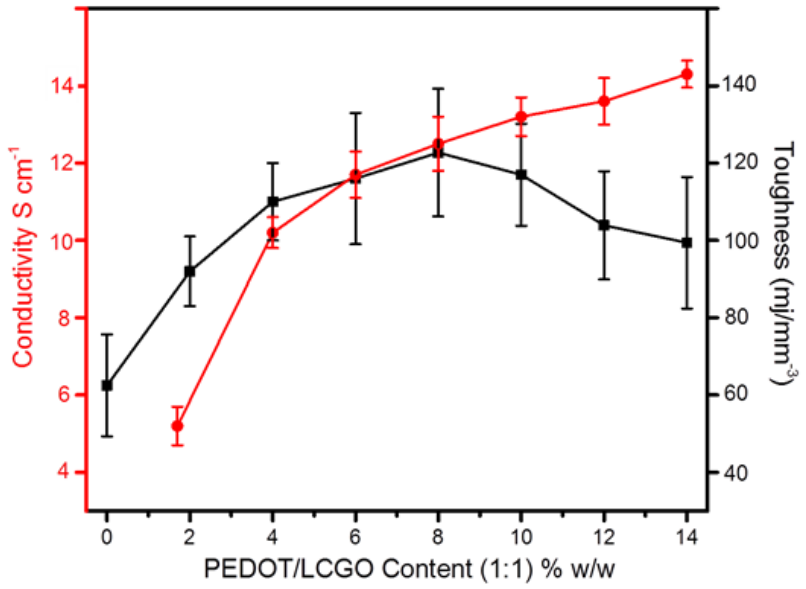

Figure 2 The toughness and conductivity of the PUHC as a function of filler (PEDOT:PSS and LCGO) loading.

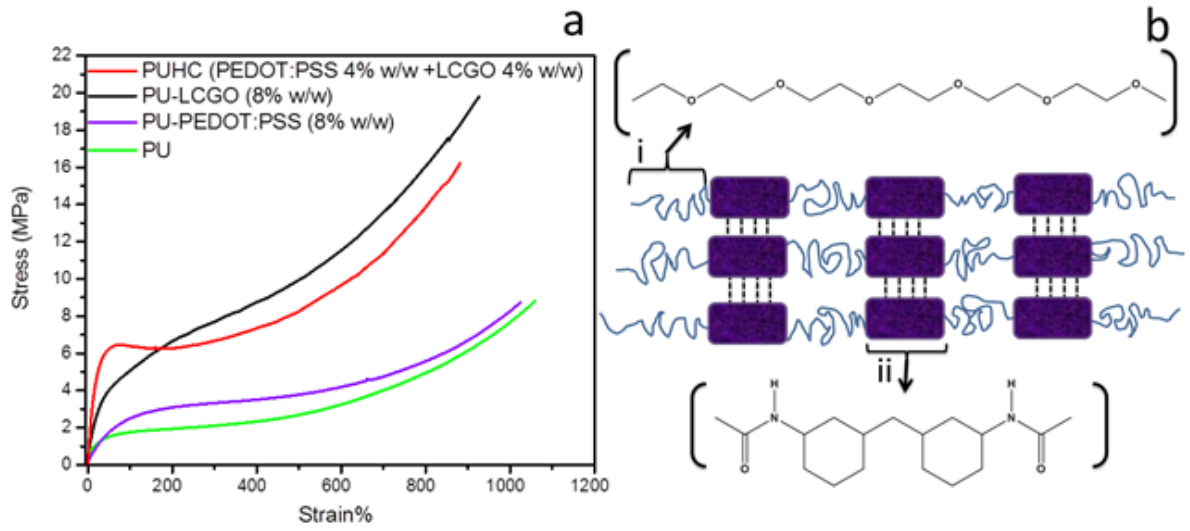

Figure 3 a) Tensile stress–strain curve of the PUHC and control samples and b) Chemical structure of PU (i: soft segment and ii: hard segment).

Table 1 The effect of fillers on the mechanical properties of PU.

	Tensile Modulus (MPa)	Ultimate Strength (MPa)	Yield Strength (MPa)	Elongation at break %	Filler % w/w*
PU	1.02 ± 0.3	7.32 ± 1.2	0.42 ± 0.12	1084 ± 96	0
PU/PEDOT: PSS	2.31 ± 0.26	10.42 ± 0.8	2.37 ±0.3	1127 ± 115	8.0*
PU/LCGO	3.45 ± 0.22	19.8 ± 1.3	3.98 ±0.24	936 ± 76	8.0*
PUHC	5.64 ± 0.34	16.21 ± 1.02	6.23 ±0.53	891 ± 93	PEDOT: PSS 4.0 LCGO 4.0

***Note:** The % w/w of the PEDOT:PSS and LCGO were chosen to be 8% in order to have the same amount of filler in these samples as is in the PUHC sample.

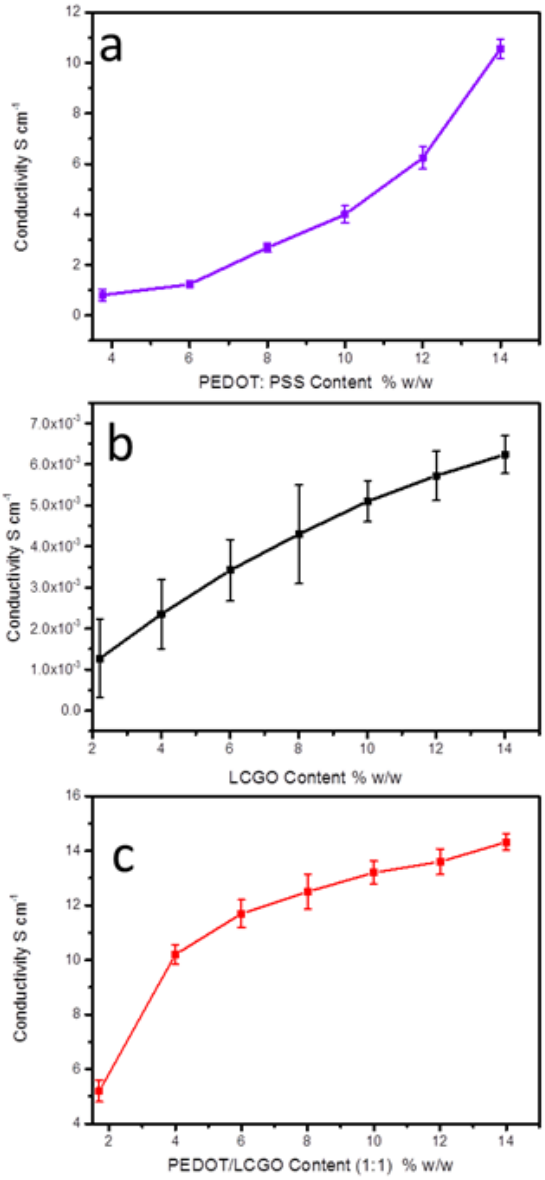

Figure 4 The electrical conductivity of PU composites containing a) PEDOT:PSS, b) reduced LCGO, and c) LCGO/PEDOT:PSS as a function of filler loading.

Table 2 Conductive PU composites with a variety of conductive fillers (data from this study and literature).

Filler	Conductivity (S/cm)	Ref.
LCGO + PEDOT: PSS (8 % w/w)	12.5	This work
PAni (34 wt%)	8×10^{-2}	[32]
PPy	10^{-7}–10^{-2}	[33]
PPy(30 wt%)	2.6×10^{-1}	[34]
MWCNTs (5 wt%)	1×10^{-3}	[35]
SWCNT + PPy (2.5wt%)	9.8×10^{-3}	[36]
Graphene (2 wt%)	10^{-5},10^{-8}	[37, 38]
Graphite (6.5 vol.%)	0.01	[39]
PEDOT: PSS (8 wt.%)	4.8	[40]

PU: Polyurethane, PPy: polypyrrole, PAni: polyaniline, MWCNT: Multi-walled carbon nanotube, and SWCNT: Single-walled carbon nanotube;

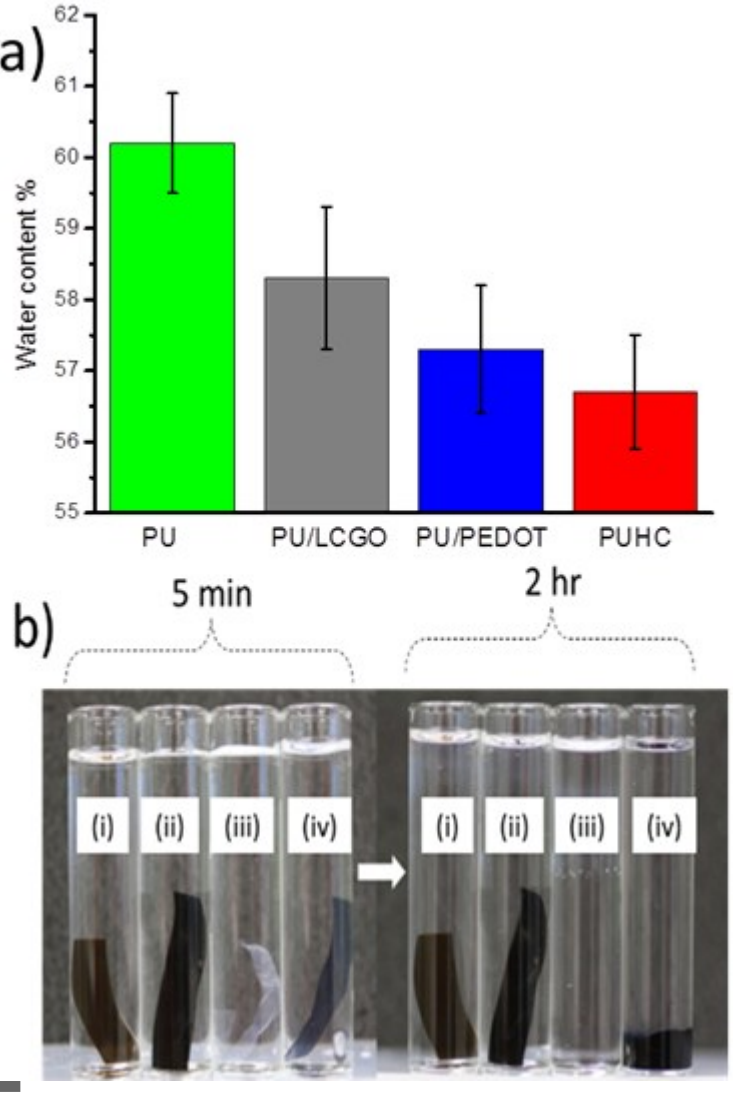

Figure 5 Water content (a) of PUHC (8 %w/w LCGO/PEDOT:PSS at 1:1), PU/LCGO (8%w/w), pure PU and PU/PEDOT: PSS (8%w/w). Photo images (b) of PUHC film (i), PU/LCGO (ii), PU (iii), and PU/PEDOT:PSS (iv) hydrogel films immersed for 5 min and 2 hr in 10 mL of EtOH-water (95-5%) solution.

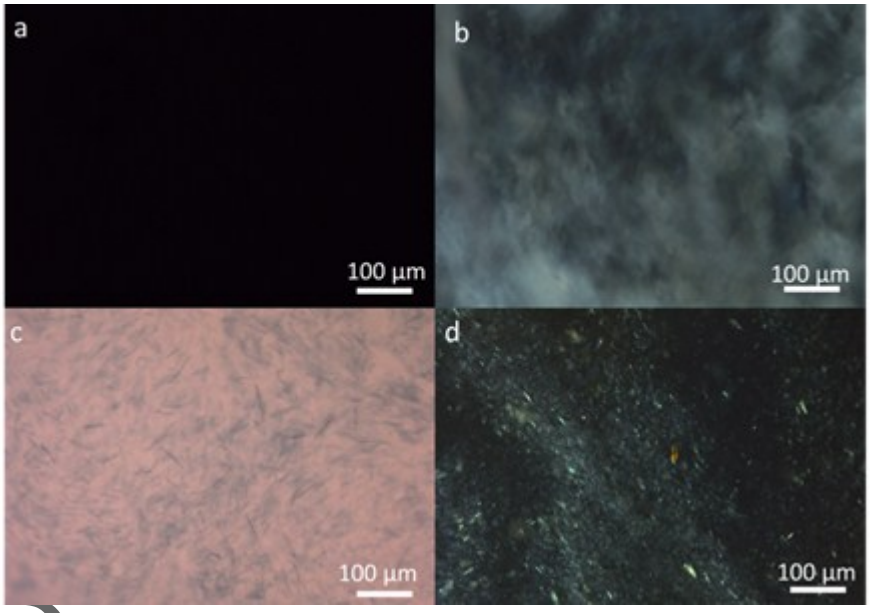

Figure 6 Representative polarized optical microscopy images of samples in solution phase. a) PU, b) LCGO (8% w/w), c) PEDOT:PSS (8% w/w) and d) PUHC (LCGO 4% w/w + PEDOT:PSS 4% w/w).

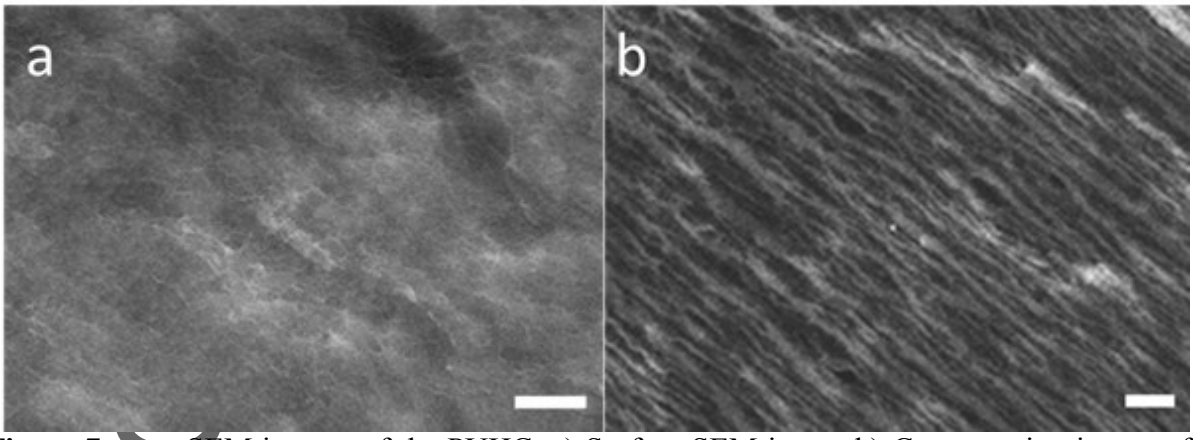

Figure 7 SEM images of the PUHC. a) Surface SEM image b) Cross-section image of PUHC. The scale bar is 10 μm.

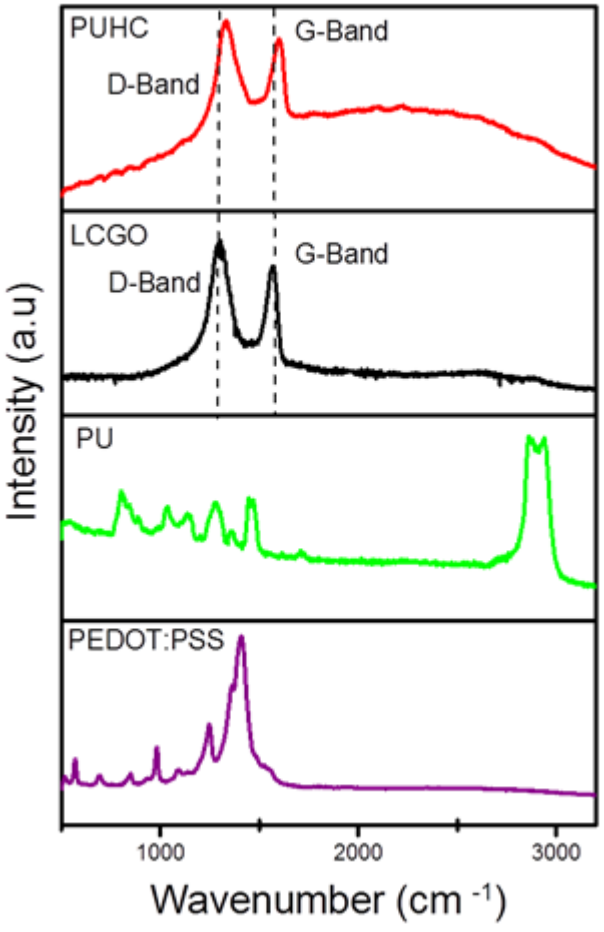

Figure 8 Raman characterization of PU, PEDOT:PSS, LCGO, and PUHC. The broken line indicates the location of D and G-band in LCGO.

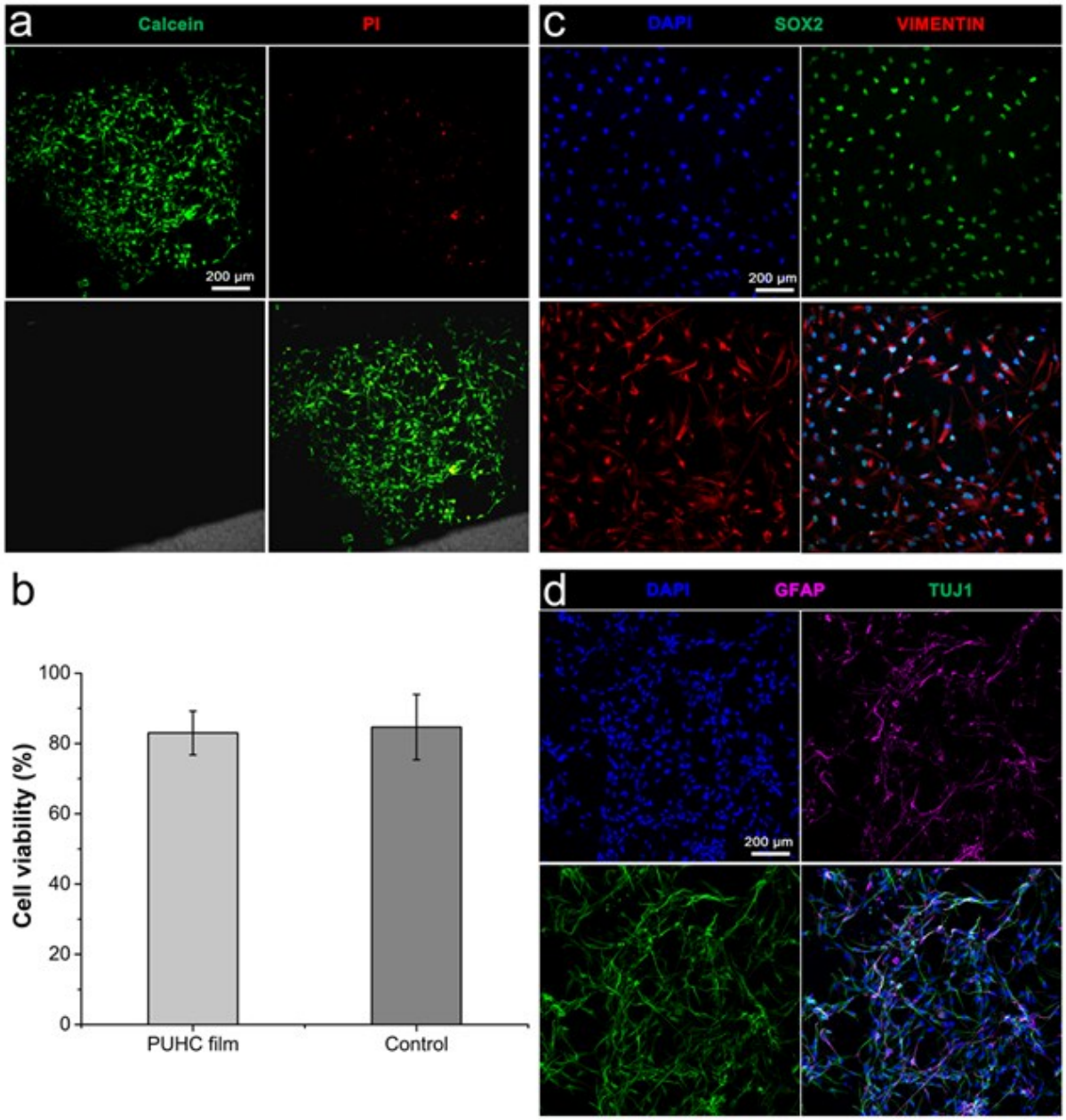

Figure 9 Survival, maintenance and differentiation of hNSCs on PUHC. (a) Live (Calcein AM) and dead (PI) cell staining following 24 h culture. (b) Quantitative analysis of hNSC viability following 24 h culture. (c) Immunocytochemistry of hNSC markers SOX2 and vimentin. (d) Immunocytochemistry of GFAP (astrocyte maker) and TUJ1 (neuronal marker) expression after differentiation of NSCs for 7 days.

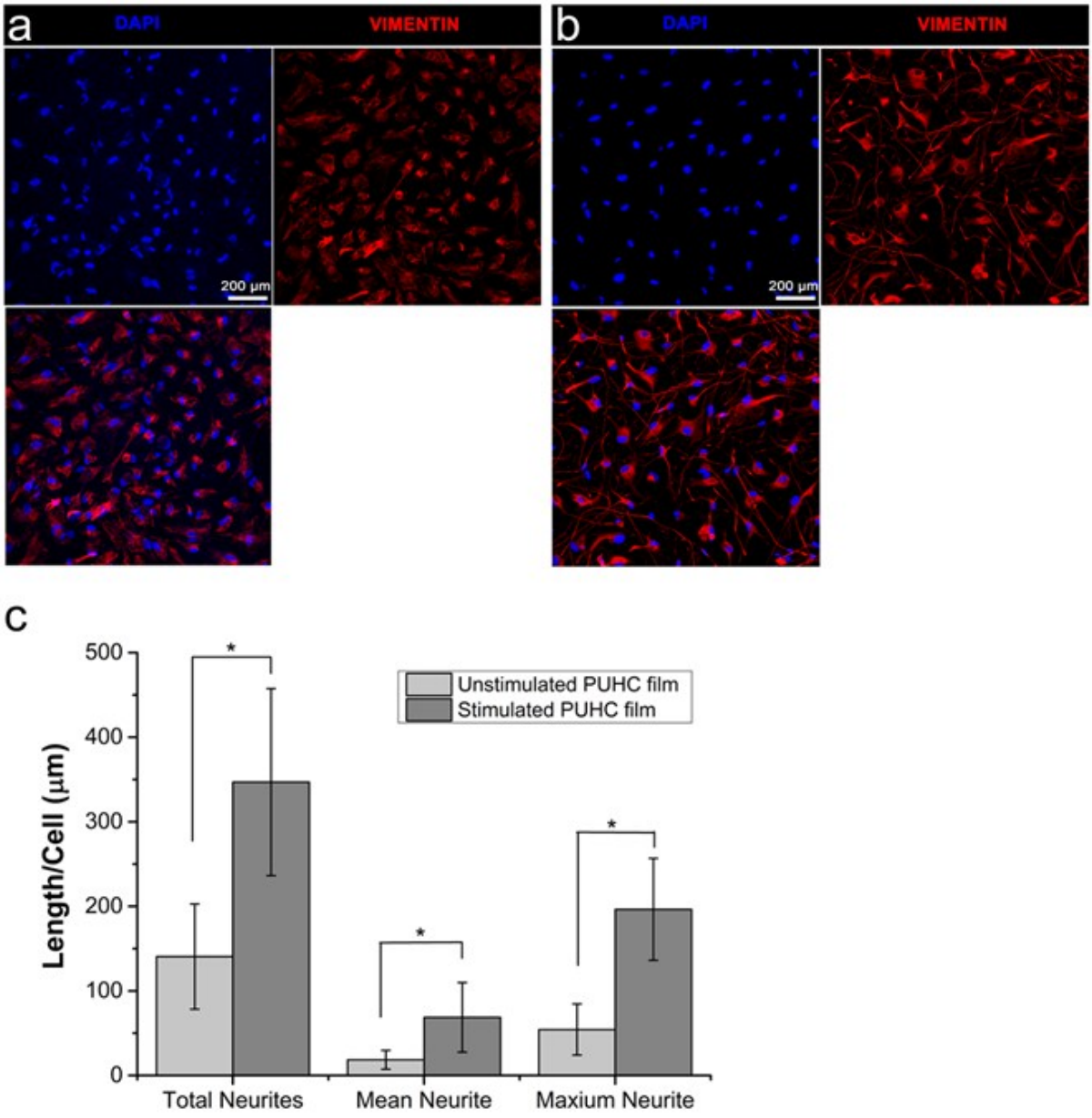

Figure 10 Neurite growth of hNSCs following culture for 3 days on PUHC with and without stimulation. (a, b) Immunocytochemistry of vimentin-expressing cells. (c) Assessment of neurite growth, including the sum total length of neurites, mean neurite length, and maximum neurite length per cell ± SD (for stimulated and unstimulated groups, n=11 and 40 respectively). ‘‘*’’ Indicates statistical significance of ≤ 0.05

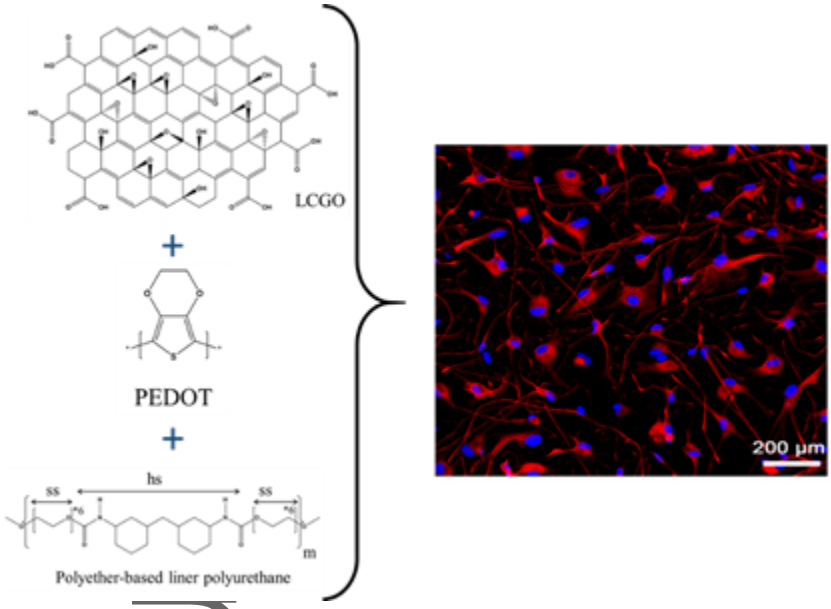

Polyurethane hybrid composite (PUHC) can support human neural stem cell (NSC) and enhances early neuritogenesis. This conductive elastomer has potential applications for mimicry of neural networks where electrical stimulation may be beneficial.